DYNAMIC CONTROL OF DEEP-LEVEL MINE COOLING SYSTEMS USING ARTIFICIAL INTELLIGENCE

M.C. Furumele[1*], J.H. Marais[2] and J.H. Van Laar[3]
[1,2,3]Centre for Sustainable Mining
North-West University, South Africa
[1]mfurumele@rems2.com, [2]jhmarais@rems2.com, [3]jvanlaar@rems2.com

ABSTRACT

Deep-level mines in South Africa face rising electricity costs, with cooling systems contributing up to 28% of a mine's total energy. Existing energy-saving approaches lack adaptability. The mining industry has rarely embraced artificial intelligence (AI)–based energy efficiency strategies. This study proposes a dynamic AI-based strategy to improve energy efficiency in deep-level gold mine cooling systems. Long-short-term memory recurrent neural network (LSTM-RNN) models are integrated into dynamic control strategies for cooling components. The strategy acquires real-time data from the mine's SCADA, forecasts temperatures, and adjusts cooling component operations, potentially saving ZAR 1.5 million annually. Advantages brought to light include reduced human error and no infrastructure changes. The results serve to motivate the struggling industry to incorporate more Industry 4.0 technologies. This study contributes to mining by providing energy savings and operational improvements, as well as to AI by indicating the effective use of AI techniques in complex industrial environments.

Keywords: mining, energy saving, dynamic control, machine learning, artificial intelligence

* Corresponding Author

1 INTRODUCTION

The mining industry in South Africa plays a major role in the country's economy [1]. Moreover, 11% of the world's gold reserves are located in South Africa, as of 2016 [2]. South African gold production has steadily declined since 1990 despite the reserves and the role that mining plays in South Africa. A graphical representation of the decline over time is displayed in Figure 1.

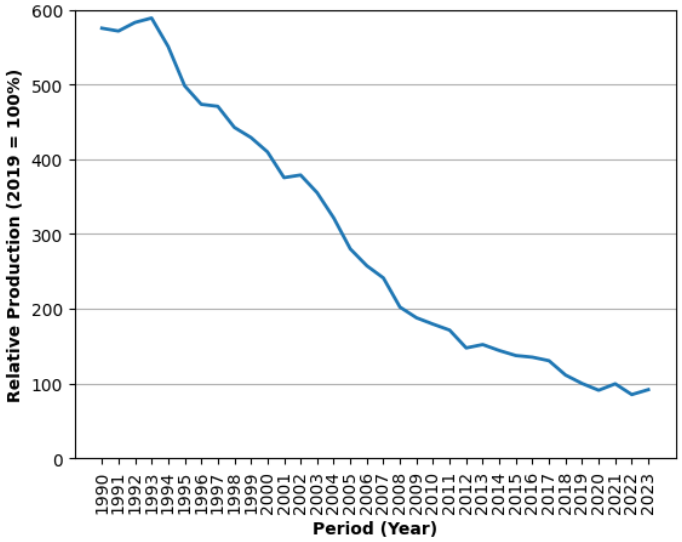

Figure 1: Gold mining historical production in South Africa [3]

The mines in South Africa are being deepened to increase their life of mine and access more gold reserves [4]. This increased depth has significantly contributed to the strain on Eskom's electricity grid [5]. Moreover, the average electricity cost in the mining industry has increased considerably each year as seen in Figure 2 [6].

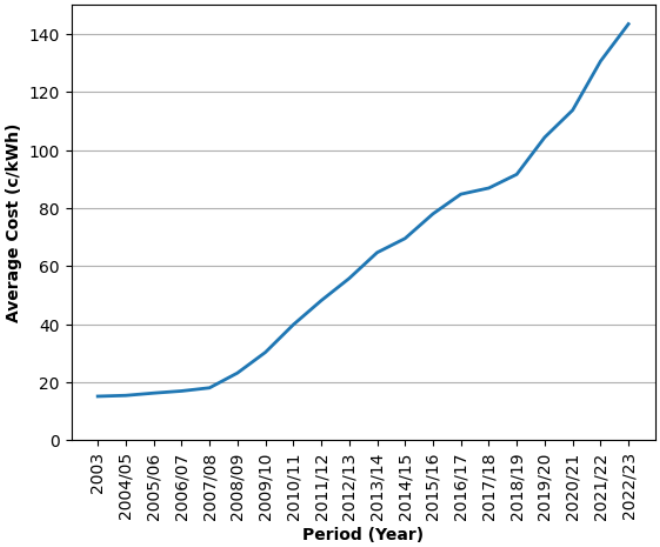

Figure 2: Electricity cost for mining in South Africa [6]

Additionally, the mining industry reduces its electricity usage during designated times to assist in maintaining a stable electricity grid thus leading to losses in production opportunities [7]. The decline in South African gold production may therefore be partially attributed to the challenges faced by deeper mines, increasing electricity costs as well as electricity supply constraints, Consequently, the implementation of energy savings initiatives can help to improve the profitability of the South African mining industry.

The main electrical energy consumers in deep-level gold mines can be observed in Figure 3 [2], [8]. Ventilation and refrigeration account for approximately 28% of the electrical energy consumption in deep-level mines [2].

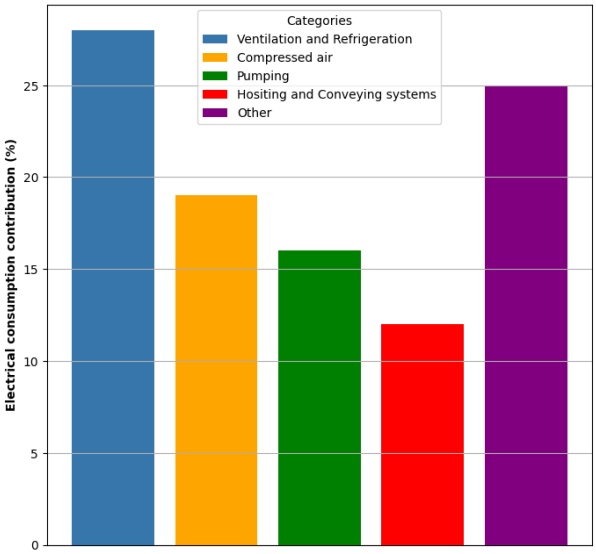

Figure 3: Typical gold mine electrical energy consumption distribution [2], [8]

Ventilation and refrigeration are typically categorised as cooling systems. Cooling systems essentially aim to reduce air temperatures in underground working areas. The air is cooled by transferring it into cold water, thus, decreasing the air temperatures in these areas [2].

South African gold mines typically reach depths of approximately 4 km and experience virgin rock temperatures (VRTs) of up to 60°C [9]. Moreover, the Mine Health Safety Act (MHSA) of South Africa prohibits working at wet bulb temperatures exceeding 32.5°C and dry bulb temperatures exceeding 37°C [10]. Therefore, cooling systems are used to mitigate the VRTs and meet the temperature regulations as set out by the MHSA of South Africa.

Typical cooling systems in deep-level mines comprise of refrigeration plants, bulk air coolers (BACs), pumps, and dams. These components are controlled to meet specific service delivery requirements, such as temperatures and dam levels [9].

In addition to meeting service delivery requirements, carrying out energy-saving strategies is crucial to address the increasing electricity costs in the mining industry. Approaches such as load shifting, peak clipping, and energy efficiency strategies are widely recognised as effective solutions for energy savings [2], [9], [11]. Table 1 indicates the use of energy savings strategies for deep-level mine cooling systems.

Table 1: Energy savings strategies for deep-level mine cooling systems [2], [9], [11]

Strategy	Description
Load shifting	Redistributing the system's energy requirements to different periods of the day while maintaining the same energy requirements and meeting cooling requirements. The shift is based on Eskom's Time-of-use (TOU) tariff structure
Peak clipping	It aims to decrease energy consumption during specific periods of the day. For cooling systems, this is frequently applied when mining personnel are not underground.
Energy Efficiency	Decreases the energy consumption while meeting the system's cooling requirements. Adjustments of control philosophies and the installation of new technologies like variable speed drives (VSD) are common implementations

The adjustments of control philosophies are commonly used for energy efficiency strategies. These are done by implementing set point control and dynamic control methods.

Set point control uses the step response method, which delivers an output to a system in response to an instantaneous event [9]. For instance, a guide vane angle is adjusted based on a predetermined angle set for a specific time of the day. This is commonly used for compressor control. Dynamic control typically considers various inputs to achieve a specific goal [12]. The response to this method is adjusted between the baseline and current operations [13]. Artificial Intelligence (AI) has shown promise in dynamic control applications [2], [14], [15].

AI is a field that encompasses numerous subjects including computer science, engineering, mathematics, and statistics [16]. However, it is often referred to as a "buzzword" and lacks a precise definition. AI is commonly defined as a resource that enhances daily human activities by various scientific committees [17].

The use of AI has become increasingly widespread across various industries for tasks that usually can operate without human intervention [18], [19]. AI applications include [16], [20], [21]:

- Automation,
- Robotics,
- Decision-making using forecasting and optimisation techniques.
- Image processing

However, the mining industry is not among the leading industries in adopting AI in its systems and processes [16]. The current nature of the data present in mining *illuminates* the potential to apply AI in the industry, specifically for decision-making [22]. Machine learning and deep learning are AI techniques commonly used for decision-making [20].

Most of the data generated in mining is time-dependent, also known as time series data. This data serves as the basis for time series forecasting. Time series forecasting aims to predict future values using time series input data [23]. This technique derives insights by examining the correlations between inputs with similar timestamps [24]. Due to the advancement of technologies and the growth of data over recent years, machine learning and deep learning techniques have increased in popularity for time series forecasting [22].

Table 2: Machine learning and deep learning techniques for time series forecasting

Model	Description
Linear regression	Identifies a linear relationship between independent and dependent variables [14], [19].
Auto-regression (AR)	Determines the future value of a variable based on its previous variable in the form of a linear formula [25].
Moving average (MA)	Linear formula based on previous average values to determine the future value of the variable [26].
Auto-regressive moving average (ARMA)	Combination of the AR and MA models.
Auto-regressive integrated moving average (ARIMA)	Modification of the ARMA, by incorporating the "integrated" section, which allows the model to predict non-stationary data [27].
Seasonal auto-regressive integrated moving average (SARIMA)	Enhances the ARIMA model by including seasonal parameters [27].

Recurrent Neural Networks (RNN)	Neural network model that uses sequential data like time series data to predict future values [28].
Gated Recurrent Unit (GRU)	Modification of the RNN, which incorporates gates to address long sequence inputs [22] [25].
Long Short-term Memory (LSTM)	Modification of the RNN, which incorporates a memory cell (gates and states) to address long sequence inputs [25].

1.1 Summary of literature

Air temperature is the primary parameter for deep-level mine cooling systems [2]. Moreover, it is a sequential measurement that varies over time, thus being categorised as time series data [29]. Therefore, it is a suitable parameter for time series forecasting.

Classical or numerical air temperature forecasting employs atmospheric models based on the existing ambient conditions [23]. This has been applied in unforeseen events like tornados, prediction of soil temperature, and energy consumption [30].

Additionally, air temperature has been an integral parameter in developing control strategies for Heating, Ventilation, and Air Conditioning (HVAC) systems in residential and office buildings [31]. Recent literature has observed that deep learning techniques are feasible for air temperature forecasting in HVAC control systems [31], [32] .

The findings of these studies indicate that LSTM-RNNs are the most common approach for air temperature forecasting. Moreover, the studies suggest that neural networks outperform traditional forecasting methods like SARIMA when handling multiple input and output parameters.

Badenhorst [33] noted that deep-level mine cooling systems are like office and residential HVAC systems, where the main parameter for their control strategies is temperature. Thus, against this backdrop, the LSTM-RNN model is the most suitable for deep-level mine cooling system control which focuses on air temperature forecasting.

LSTM-RNN models can identify patterns from input variables over a long sequence [25]. As mentioned in Table 2, the LSTM model incorporates a memory cell. The memory cell is divided into two segments. The first segment contains an input gate, a forget gate, and an output gate. Usually, the multilayer perceptron (MLP) serves as the output gate. The second segment contains a cell state and a hidden state.

MLP is the most common and simplest form of an Artificial Neural Network (ANN) [28]. ANNs are seen as representations of complex mathematical equations [34]. Its structure is based on neurons, like those in the human brain [14], [35]. The neurons are interconnected and communicate with each other, forming a network enabling it to derive insights from the communication channel [36]. Figure 4 illustrates the basic architecture of an ANN feed-forward network.

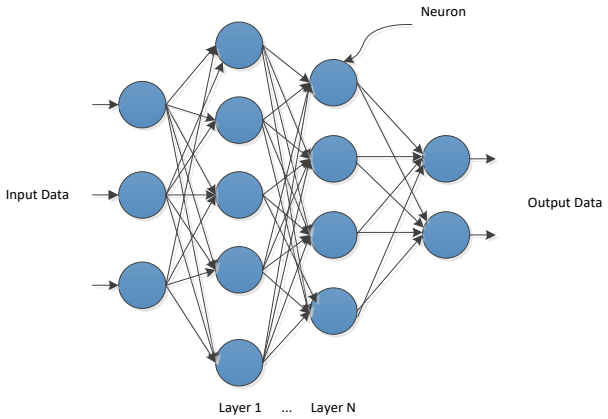

Figure 4: ANN architecture (adapted from [36])

MLP is a feed-forward network [32], [37]. A feed-forward network is an ANN where information flows in one direction.

The gates of the LSTM determine which data is important for the model. The states are used for collecting data for the next time step [22]. These segments are integral for gathering insights from the data for accurate forecasting.

The input, forget, and output gates are described mathematically in Equations *(1)*, *(2)*, and *(3)*. The hidden, cell, and new state are given by Equations *(4)* and *(5)*. The structure of the LSTM memory cell is illustrated in Figure 5.

$$i_t = \sigma\left(W_i h_{(t-1)} + W_i h_t\right) \quad \textbf{(1)}$$

$$f_t = \sigma\left(W_f h_{(t-1)} + W_f h_t\right) \quad \textbf{(2)}$$

$$o_t = \sigma\left(W_o h_{(t-1)} + W_o h_t\right) \quad \textbf{(3)}$$

$$C = tanh\left(W_c h_{(t-1)} + W_c h_t\right) \quad \textbf{(4)}$$

$$c_t = (i_t C) + \left(f_t c_{(t-1)}\right) \quad \textbf{(5)}$$

Here:

- i_t is the input gate
- σ is the sigmoid function
- W_i, W_f, W_o, and W_c are the parameter matrices for each of the gates and states
- h_t is the new state or output vector
- f_t is the forget gate
- o_t is the output gate
- C is the hidden cell state
- c_t is the cell state

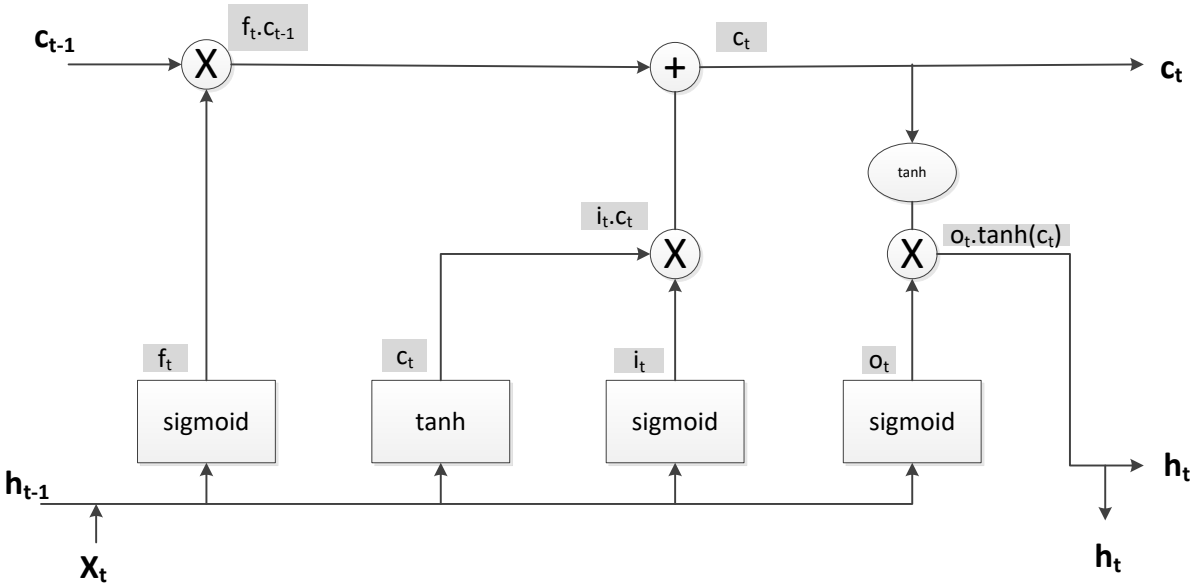

Figure 5: LSTM cell structure (adapted from [22])

Here:

- X_t is the input vector or variable

Existing literature indicates that traditional control strategies have been implemented successfully for deep-level mine cooling systems [9], [11], [33]. However, some of the studies required the installation of additional infrastructure for their control strategies [9]. Moreover, some of the implemented strategies lack adaptability [11], [33]. Cooling systems depend on dynamic conditions, like underground air temperatures. AI-inspired forecasting methods have shown the ability to forecast these conditions [31], [32].

1.2 Study objectives

This paper is based on the research conducted for the M.Eng dissertation completed at the North-West University in 2023 by Furumele [38]. The study aims to develop a dynamic control strategy for deep-level mine cooling systems using AI-inspired temperature forecasting. A case study research methodology is employed to evaluate the strategy on a deep-level gold mine cooling system. Key parameters related to the cooling system are identified and used to develop and evaluate a temperature forecasting model, which forms the basis for the dynamic control solution on the cooling system.

Furthermore, the study aims to contribute to mining research by implementing a control strategy that achieves energy savings in the mining environment and to the field of AI by applying AI techniques in complex industrial settings.

2 DYNAMIC CONTROL STRATEGY DEVELOPMENT

This study focuses on developing a dynamic control strategy for a section of a deep-level gold mine cooling system in South Africa. Additional information regarding the dynamic control strategy methodology can be observed in Furumele [38]. The overview of the methodology is illustrated in Figure 6

Figure 6: Methodology development overview

The mine, extending to a depth of 3 700 m and containing 15 working levels, uses a surface cooling system to reduce water temperature before it is transported underground. Due to the high VRTs at the mine's depths, additional cooling from smaller systems such as BACs and cooling cars is used to ensure reduced air temperatures in the working areas.

The surface cooling system is illustrated in Figure 7. The system contains three fridge plants (FPs) two ammonia plants (APs), and an optional cooling plant, which includes BAC ammonia plants (BAC APs). Hot water is pumped from underground to the pre-cooling dam, then it passes through the pre-cooling towers before being sent to the FPs for initial cooling of the hot water.

The water then moves to the intermediate dam and the APs for additional cooling. The BAC APs draw water from the intermediate dam send the water to the BAC and return it to the intermediate dam. Additionally, the APs and the BAC APs send cold water to the chill dam. Subsequently, the water from the chill dam is sent underground. This study will focus on the BAC APs and the BAC.

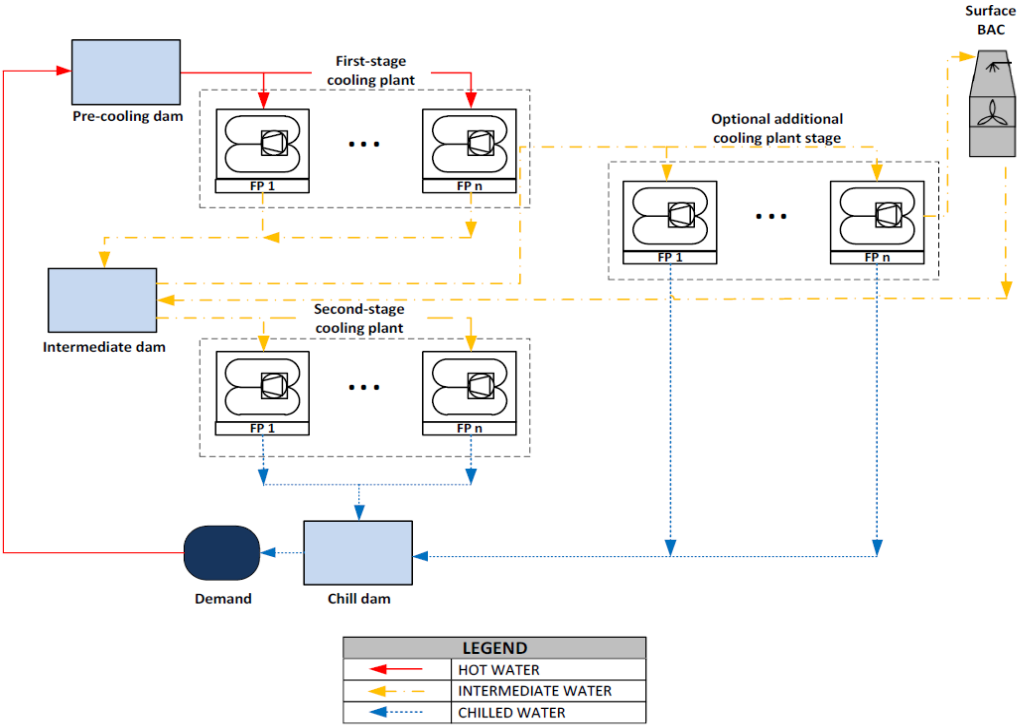

Figure 7: Multi-stage cooling system with the option for additional cooling [11]

2.1 System parameter identification

The study is limited to the BAC APs, the BAC, and a specific working area to avoid scope creep and reduce model complexity. Key parameters, including the surface and underground temperatures, BAC AP power consumption, BAC AP and BAC fan running statuses, and additional cooling auxiliaries were determined from the SCADA system. These parameters, primarily, the temperatures, form the basis of the dynamic control solution and can be adjusted during the temperature forecasting model development.

2.2 LSTM-RNN model development

The LSTM-RNN model is developed to forecast surface and underground air temperatures. The model is developed in Python using the Keras, Pandas, NumPy, and Scikit-Learn libraries. Various models are developed to forecast towards different horizons, such as forecasting one day (48 timesteps) in advance. The following models are developed:

- Model A: trained to forecast 48 timesteps (30-minute intervals) in advance.
- Model B: trained to forecast 24 timesteps (30-minute intervals) in advance.
- Model C: trained to forecast 4 timesteps (30-minute intervals) in advance, yielding a mean absolute percentage error (MAPE) of 10% on the test set.
- Model D: trained to forecast 2 timesteps (30-minute intervals) in advance, yielding a mean absolute percentage error (MAPE) of 5% on the test set.
- Model E: trained to forecast 1 timestep (30 minutes) in advance.

Figure 8 details the steps required to develop and evaluate the model [38]:

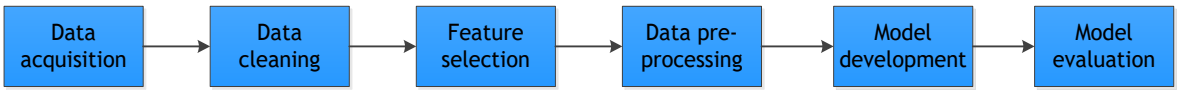

Figure 8: LSTM-RNN model development steps [38]

2.2.1 Step 1: Data acquisition

Data from the mine's historian database is extracted in 30-minute intervals using SQL queries. Each SQL query selects the "*TagName*", "*DateTime*", and "*Value*" from the database. Each parameter is represented as a tag ("*TagName*" and "*Value*") and extracted by specifying the date interval ("*DateTime*"). The data is aggregated in 30-minute intervals. This query is repeated for each parameter that is relevant to mine's cooling system and saved in a CSV file for further analysis and modelling.

2.2.2 Step 2: Data cleaning

The data that is extracted from the previous step is in its raw format and requires transformation for the subsequent steps of the model development. The data cleaning process includes the removal of outliers and the handling of missing data. The outliers were detected by examining the parameter's normal operating ranges. After examination, the identified outliers are removed from the dataset.

The missing data is handled using K-nearest neighbours (KNN) imputation. KNN imputation uses the *"K"* closest data points (neighbours) to determine what the missing data would be. The five closest data points are used to identify the missing values and can be adjusted if model improvement is required.

2.2.3 Step 3: Feature selection

Feature selection identifies the most relevant parameters that are suitable for forecasting the temperatures. Additional parameters can be incorporated if the model's performance is inadequate. The following parameters are determined as inputs for the model development:

- Surface ambient wet bulb air temperature (°C)
- Surface ambient dry bulb air temperature (°C)
- Hour of the day
- Day of the month
- Month of the year
- 7 Level air wet bulb temperature (°C)
- 7 Level air dry bulb temperature (°C)

2.2.4 Step 4: Data pre-processing

Further transformations of the data need to be implemented to ensure that the data is suitable for the LSTM-RNN model. Sliding window implementation, data partitioning, and data scaling are the techniques that will need to be implemented.

The sliding window represents the number of previous time values to forecast the next output value. For instance, model A uses 48 previous timesteps to forecast the value 48 timesteps ahead. The window "slides" to the next position to forecast the next output values.

Data partitioning divides the dataset into training, validation, and test sets. Model training uses the training set and the model's performance is evaluated using the validation set. After training, the model's performance is further evaluated using the test set. The dataset is divided such that 80% of the dataset is the training set, 5% is the validation set, and 15% is the test set.

The data is now scaled to improve the performance of the model during training, especially if the parameters' values differ drastically. The min-max scaling method is commonly used as a scaling method for neural network models and can be observed in Equation (6) [36].

$$x_{i_{scaled}} = \frac{x_i - x_{min}}{x_{max} - x_{min}} \quad \textbf{(6)}$$

2.2.5 Step 5: Model development

The model can now be developed after all the data has been transformed from its raw format to the model's desired format. The following hyperparameters are determined for all the models:

- Hidden layer activation function: LSTM (hidden layer)
- Output layer activation function: Linear
- Number of neurons: 7 (input layer), 32 (hidden layer), and 4 (output layer)
- Number of epochs: 300
- Callback function: Model checkpoint (saves the best performance to avoid overfitting)
- Batch size: 32
- Learning rate: 0.0001

The model is trained based on these hyperparameters using the training set and then verified using the validation set. After training both sets are evaluated using the coefficient of variation for the root mean square error (CV(RMSE)), the root mean square error (RMSE), and MAPE described in Equations:

$$CV(RMSE)\% = \sqrt{\frac{\frac{1}{N}\sum_{i=1}^{N}(y_i - \hat{y}_i)^2}{\bar{y}}} \times 100 \quad \textbf{(7)}$$

$$RMSE = \sqrt{\frac{\sum_{i=1}^{N}(y_i - \hat{y}_i)^2}{N}} \quad \textbf{(8)}$$

$$MAPE = \frac{\sum_{i=1}^{N}|y_i - \hat{y}_i / y_i|}{N} \times 100 \quad \textbf{(9)}$$

Here:

- N is the number of parameters.
- y_i is the actual value.
- $\hat{y}_i$ is the predicted value.
- $\bar{y}$ is the mean value of the actual values.

2.2.6 Step 6: Model evaluation

After model training, the models are evaluated based on their ability to forecast surface and underground temperatures to determine if they are suitable for a dynamic control strategy. According to ASHRAE Guideline 14, an acceptable CV(RMSE) value for model performance below 5% for half-hourly data is acceptable [39]. A maximum value of 10% for the MAPE is considered acceptable for the models [14], [34], [11]. The RMSE value will indicate whether the models are overfitting [14].

2.3 Dynamic control strategy

The model is ready to be implemented into the dynamic control strategy after the model has undergone training and evaluation. The model makes forecasts based on real-time data. This data will need to undergo the same data transformations that were done during the model training phase.

The control strategy will be used to pinpoint periods of the day when the surface BAC APs and fans may not be required to be operational. The basic flow diagram can be observed in Figure 9. The strategies that are determined will be based on the temperature forecasting models that were developed. The models that are insufficient in terms of performance will be disregarded. Thus, decreasing the number of solutions.

Figure 9: Dynamic control solution overview [38].

The following specifications form the basis of the control strategy [38]:

- Specification 1: Data gathering.
- Specification 2: Temperature forecasting.
- Specification 3: System operations suggestion.

The real-time data is extracted in half-hourly periods and undergoes the same transformations that were done during model development. Once the data is in the correct format, the temperatures are forecasted and evaluated against temperature targets.

The target for the surface air wet-bulb temperature is **7°C**, which is based on a previous study that implemented a seasonal control strategy on the surface cooling system. The 7 level air wet bulb temperature target is **32°C**, which is based on the MHSA of South Africa's underground temperature requirements. Against this backdrop, the operation suggestion is determined based on these target temperatures.

3 RESULTS AND DISCUSSION

3.1 Model development results

As discussed in Section 2.2, Five models were developed with varying forecasting horizons. The model performance after training can be seen in Figure 10.

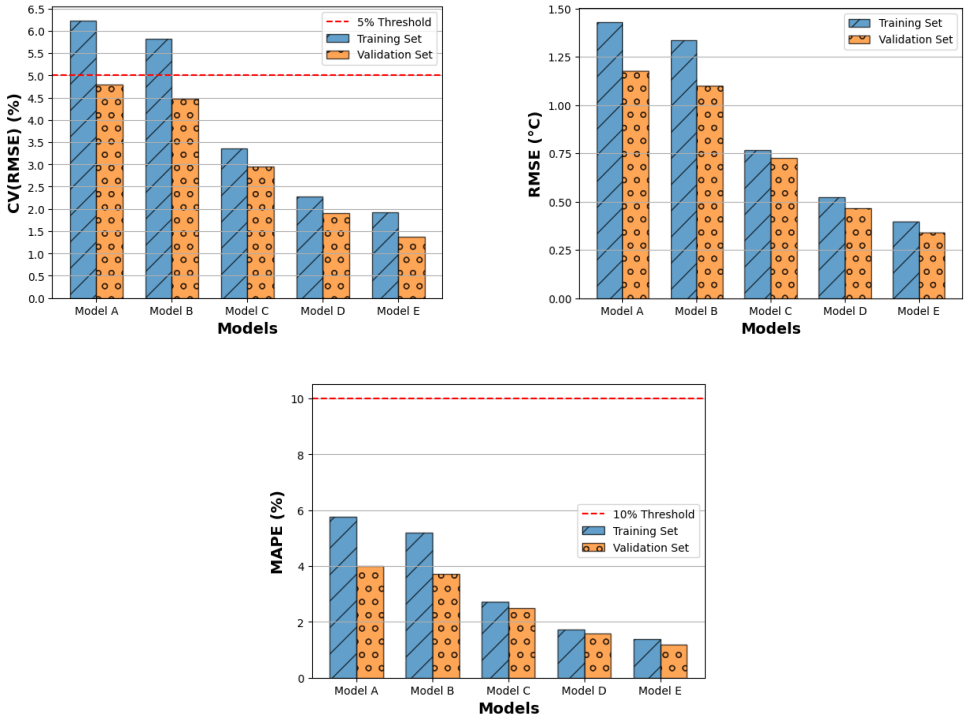

Figure 10: CV (RMSE), RMSE, and MAPE values for the training and validation sets [38].

Based on Figure 10, the validation sets exhibit lower values than the training sets for all the above metrics. Thus, this suggests that the models can predict well on unseen data. Moreover, the metrics show that the model improves for smaller forecasting horizons.

The true performance needs to be evaluated using the test set which is not involved during the model training phase. The model performance based on the test set indicates whether the models can predict temperatures on new and unseen data. The CV(RMSE) and MAPE values can observed in Figure 11. The results show the same trend observed in Figure 10, where values improve as the forecasting horizons decrease. The model is less likely to include irregular data points as inputs for predictions for smaller horizons. Thus, improving the model performance.

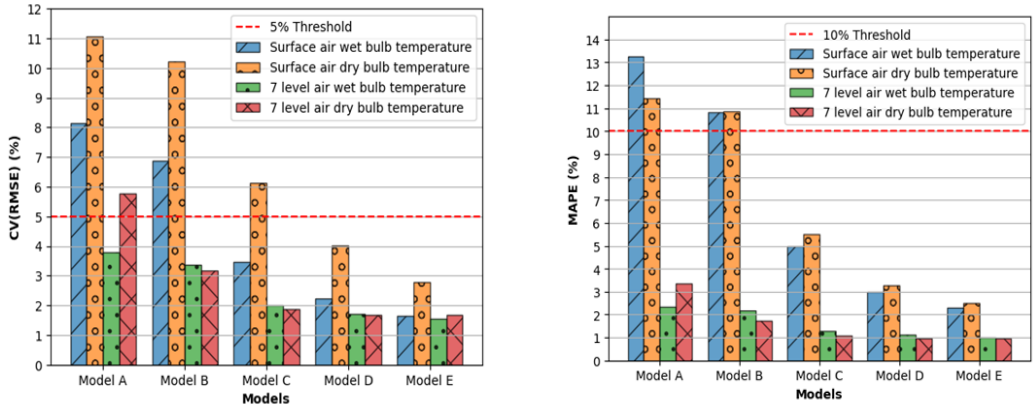

Figure 11: CV(RMSE) and MAPE values for the test set [38].

Models D and E attained CV(RMSE) values below the 5% threshold for all forecasted temperatures. Additionally, Models C, D, and E achieved MAPE values below the 10% threshold for all forecasted temperatures. Although Model C achieved a value above the 5% threshold for the surface air dry bulb temperature (6.12%). Model C is still considered an accurate model since the wet bulb temperatures are crucial for the dynamic control strategy instead of the dry bulb temperatures. Consequently, Models C, D, and E are deemed accurate for temperature forecasting.

3.2 Dynamic control solution

The dynamic control solution was developed based on specifications detailed in Section 2.3 and Figure 9. Models C (two-hour forecast), D (one-hour forecast), and E (30-minute forecast) were used to develop the strategies.

Real-time data was extracted to be used for the chosen models. The amount of data (periods) extracted depended on what was required to forecast the temperatures.

For instance, Model D requires data from the previous hour and the present time to forecast the next two timesteps (30-minute intervals).

The extracted data was transformed using the same procedure used during model training. However, data partitioning is excluded from the transformations. Figure 12 shows the real-time wet bulb temperature forecasts.

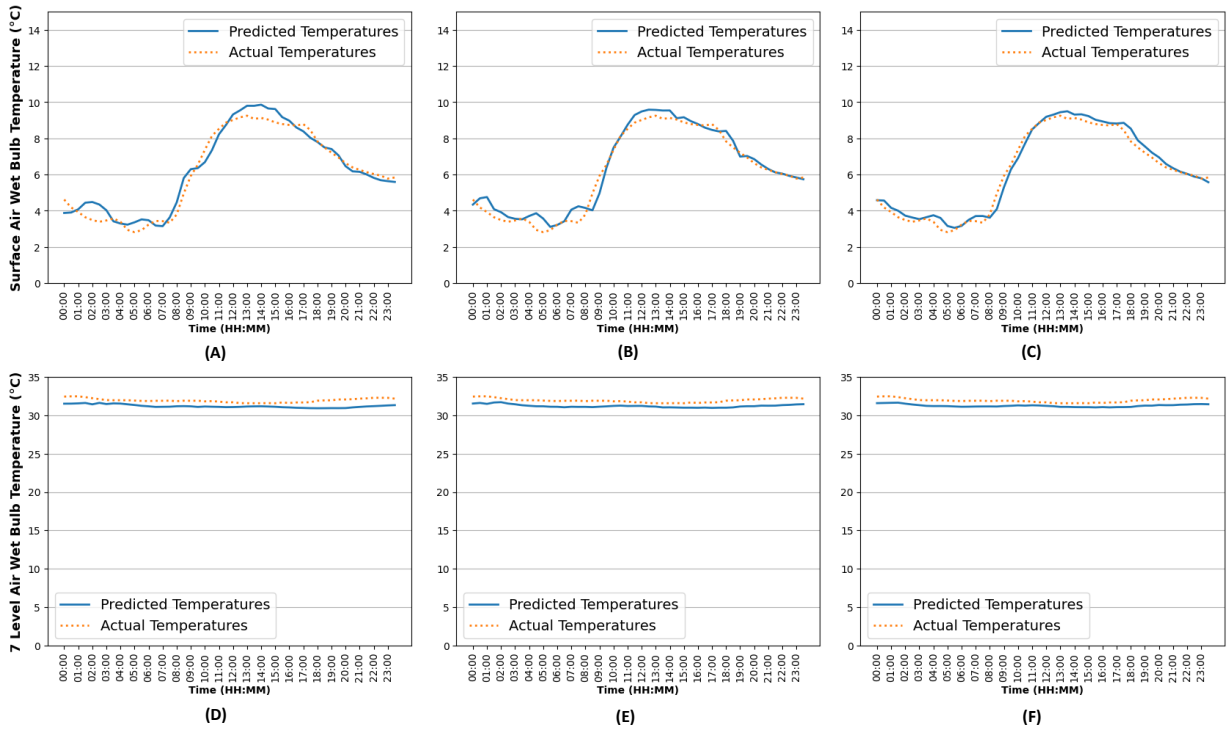

Figure 12: Real-time forecast of the surface and 7 level air wet bulb temperatures using model C [(A) and (D)], model D [(B) and (E)], and model E [(C) and (F)] [38].

From the observations, the forecasting accuracy improves later in the day since it becomes less dependent on the previous day's data. Moreover, there is less variation in the underground temperatures compared to the surface temperatures, due to the additional cooling auxiliaries underground. Table 3 details the MAPE values for the real-time temperature forecasts.

Table 3: MAPE (%) values for real-time temperature forecasts [38].

Parameter	Model C	Model D	Model E
Surface air wet bulb temperature	7.72	6.57	4.9
Surface air dry bulb temperature	6.36	4.02	3.41
7 level air wet bulb temperature	2.32	2.27	2.14
7 level air dry bulb temperature	2.25	2.28	2.37

The MAPE values are below the 10% threshold for all the temperatures, thus indicating that the models are accurate. These models form the basis of the dynamic control solutions. Temperature targets of 7°C for the surface air wet bulb temperature and 32°C for the 7 level air wet bulb temperatures are used to determine whether BAC APs and fans need to operate based on the temperature forecasts.

The dynamic control solution was implemented for a day in the summer months and the winter months (June, July, and August). The real-time forecasted temperatures on a day in the summer months are detailed in Figure 13.

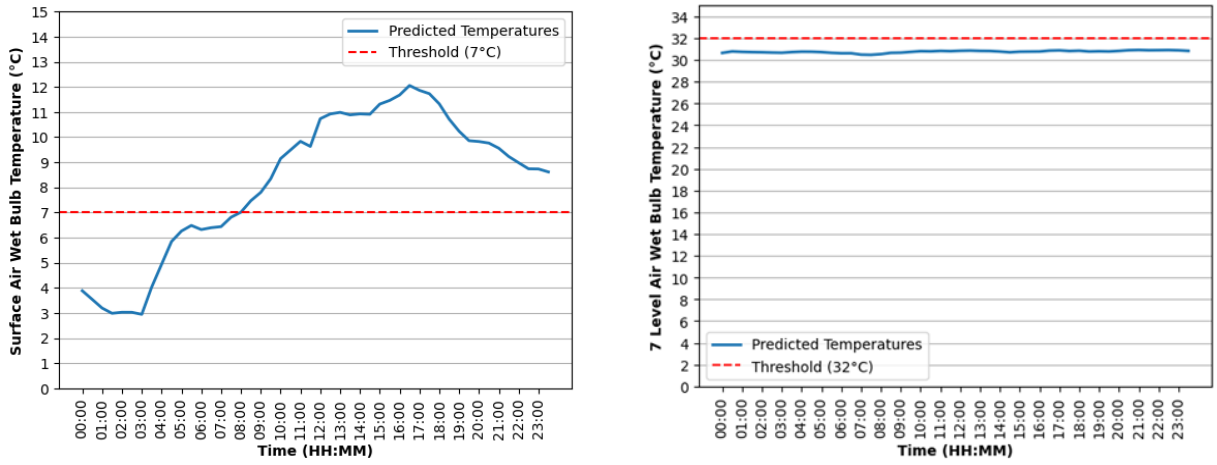

Figure 13: Forecasted summer surface and 7 level air wet bulb temperatures using model E [38].

MAPE values of 3.75% and 1.42% were achieved for the summer months. The surface temperatures were below the 7°C threshold between 00:00 and 08:00 and were below the 32°C threshold for the 7 level temperatures for the whole day. Therefore, the temperatures suggest that the BAC APs and fans can be switched off between 00:00 and 08:00.

However, this is under the assumption that the additional cooling auxiliaries remain constant throughout the day. The real-time forecasted temperatures on a day in the winter months are detailed in Figure 14.

MAPE values of 6.82% and 2.31% were achieved during the winter months. The BAC APs and fans can be switched off all day since the surface temperatures are slightly above the 7°C threshold (peak = 7.11°C) and below the 32°C threshold.

Model C achieved MAPE values of 13.81% and 2.80% and Model D achieved MAPE values of 8.26% and 2.68%, respectively. These values are for the surface and 7 level air wet bulb temperatures. Model D was the most suitable for the dynamic control solution. Model C is most likely to yield inaccurate forecasts. Although Model E is the best-performing model, Model D

gives the mine sufficient lead time to prepare to change the operating status of BAC APs and fans.

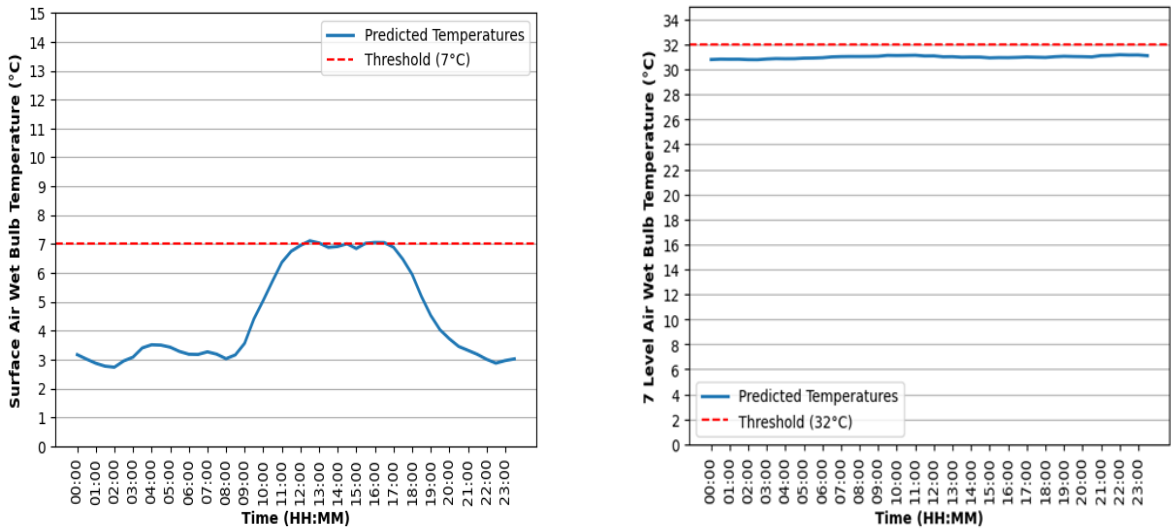

Figure 14: Forecasted winter surface and 7 level air wet bulb temperatures using model E [38].

Electricity cost savings were calculated to assess whether the dynamic control strategy leads to a reduction in electricity usage. A potential electricity cost savings of ZAR 1.5 million per annum are projected with a reduction in electricity of 20 MWh in 2023. The cost savings were calculated using 2022/2023 Eskom tariffs. Most of the savings were observed during the transitional months between the seasons (May and September).

4 CONCLUSION

Existing deep-level mine cooling system strategies lack adaptability based on dynamic conditions. AI *illuminates* the potential to address dynamic control strategies. This study developed a dynamic control strategy for a deep-level mine cooling system, specifically the BAC APs and fans. An LSTM-RNN temperature forecasting model formed the basis of the control strategy. The model was used to forecast temperatures across various horizons and was used to identify suitable operating conditions for the BAC APs and fans.

4.1 Limitations and Recommendations

The models that were developed were able to forecast temperatures accurately. However, they did tend to struggle for longer forecasting horizons (more than 2 hours). It is important to consider applying other forecasting techniques such as GRU and CNN techniques, which could yield better results for the longer horizons. However, the chosen model will improve with additional data.

Moreover, the strategy should be implemented as an automated real-time solution with a model that contains smaller forecasting horizons (30 minutes or less) for BAC APs and fans. Additionally, the solution can be integrated into a holistic control strategy for the entire cooling system.

5 REFERENCES

[1] K. B. Sesele, "Women and Mining Decline in the Free State Goldfields," PhD Thesis, University of the Free State, Bloemfontein, 2020.

[2] M. D. Harmse, "Optimising mining refrigeration systems through artificial intelligence," M.Eng Dissertation, North-West University, Potchefstroom, 2021.

[3] "Statistics South Africa: Mining; Production and Sales, February 2024," 11 April 2024. [Online]. Available: https://www.statssa.gov.za/?page_id=1854&PPN=P2041. [Accessed 22 April 2024].

[4] "Department of Mineral Resources and Energy: New Technological Applications in Deep-level Gold Mining," 2013. [Online]. Available: https://www.dmr.gov.za/LinkClick.aspx?fileticket=CIEuCiHYXlA%3D&portalid=0. [Accessed 11 November 2023].

[5] P. Mare, "Novel simulations for energy management of mine cooling systems," PhD Thesis, North-West University, Potchefstroom, 2017.

[6] Eskom, "Tariff History," 2024. [Online]. Available: https://www.eskom.co.za/distribution/tariffs-and-charges/tariff-history/. [Accessed 19 May 2024].

[7] C. Caromba, C. Schutte and J. van Laar, "Application of Clustering Techniques for Improved Energy Benchmarking on Deep-Level Mines," Energies, vol. 16, p. 6879, 2023.

[8] W. G. Shaw and M. M. J. Mathews, "Holistic analysis of the effect on electricity cost in South Africa's platinum mines when varying shift schedules according to time-of-use shifts," Journal of Energy in Southern Africa, vol. 30, no. 4, pp. 26-40, 2019.

[9] J. A. Crawford, H. P. R. Joubert, M. J. Mathews, and M. Kleingeld, "Optimised dynamic control philosophy for improved performance of mine cooling systems," Applied Thermal Engineering, vol. 150, pp. 50-60, 2019.

[10] " MHSA of South Africa: Mine Health and Safety Act 29 of 1996 and Regulations," 2018.

[11] J. Lodewyk, "Holistic evaluation of surface cooling plant configurations for different seasons at deep mines," M.Eng Dissertation, North-West University, Potchefstroom, 2022.

[12] Woolf, Chemical Process Dynamics and Controls, Michigan: University of Michigan Engineering Controls Group, 2009.

[13] R. C. Ilambirai, P. Sivasankari, S. Padmini and H. Chowdary, "Efficient Self-Learning Artificial Neural Network Controller for Critical Heating, Ventilation and Air Conditioning Systems," in AIP Conference Proceedings, 2019.

[14] G. J. Mathee, "Improved control of compressed air networks using machine learning," M.Eng Dissertation, North-West University, Potchefstroom, 2021.

[15] Z. Hyder, K. Siau and F. Nah, "Artificial intelligence, machine learning, and autonomous technologies in the mining industry," Journal of Database Management (JDM), vol. 30, no. 2, pp. 67-79, 2019.

[16] W. Wang and K. Siau, " Artificial intelligence, machine learning, automation, robotics, future of work and future of humanity: A review and research agenda," Journal of Database Management (JDM), vol. 30, no. 1, pp. 61-79, 2019.

[17] P. M. Kraft, M. Young, M. Katell and B. G. Huang, "Defining AI in Policy versus Practice," in AIES '20: Proceedings of the AAAI/ACM Conference on AI, Ethics, and Society, 2020.

[18] J. Bughin, E. Hazan, S. Ramaswamy, M. Chui, T. Allas, P. Dahlstrom, N. Henke, and M. Trench, "Artificial intelligence: the next digital frontier?," McKinsey Global Institute, 2017.

[19] I. O. Olayode, B. Du, L. K. Tartibu and F. J. Alex, "Traffic flow modelling of long and short trucks using a hybrid artificial neural network optimized by particle swarm optimization," International Journal of Transportation Science and Technology, vol. 14, pp. 137-155, 2024.

[20] K. K. Ng, C.-H. Chen, C. K. M. Lee, J. Jiao and Z.-X. Yang, "A systematic literature review on intelligent automation: Aligning concepts from theory, practice, and future perspectives," Advanced Engineering Informatics, vol. 47, p. 101246, 2021.

[21] S. Robertson, H. Azizpour, K. Smith and J. Hartman, "Digital image analysis in breast pathology - from image processing techniques to artificial intelligence," The Journal of Laboratory and Clinical Medicine, vol. 194, pp. 19-35, 2018.

[22] P. Yamak, L. Yujian and P. K. Gadosey, "A Comparison between ARIMA, LSTM, and GRU for Time Series Forecasting," in Proceedings of the 2019 2nd International Conference on Algorithms, Computing and Artificial Intelligence, Sanya, 2019.

[23] P. Chen, N. Aichen, L. Duanyang, W. Jiang and B. Ma, "Time Series Forecasting of Temperatures using SARIMA: An Example from Nanjing," IOP Conference Series: Materials Science and Engineering, vol. 394, no. 5, p. 052024, 2018.

[24] R. Shumway and D. Stoffer, Time Series Analysis and Its Application with R Examples, New York: Springer, 2011.

[25] A. Alsharef, K. Aggarwal, M. Kumar and A. Mishra, "Review of ML and AutoML Solutions to Forecast Time Series Data," Archives of Computational Methods in Engineering, pp. 1-15, 2022.

[26] R. J. Hyndman, International Encyclopedia of Statistical Science: Moving Averages, Springer, 2010.

[27] C. S. Fiskin, O. Turgut, S. Westgaard, and A. Cerit, "Time series forecasting of domestic shipping market: comparison of SARIMAX, ANN-based models and SARIMAX-ANN hybrid model," International Journal of Shipping and Transport Logistics, vol. 14, no. 3, pp. 193-221, 2022.

[28] T. T, S. Bateni, S. Ki and H. Vosoughifar, "A Review of Neural Networks for Air Temperature Forecasting," Water 2021, vol. 13, no. 9, pp. 1294-1309, 2021.

[29] R. J. Hyndman and G. Athanasopoulos, Forecasting: principles and practice, OTexts, 2018.

[30] M. Afzali, A. Afzali, and G. Zahdei, "Ambient Air Temperature Forecasting Using Artificial Neural Network Approach," in International Conference on Environmental and Computer Science, Singapore, 2011.

[31] P. Hietaharju, M. Ruusunen and K. Leiviskä, "A Dynamic Model for Indoor Temperature Prediction in Buildings," Energies, vol. 13, no. 12, 2018.

[32] X. Godinho, H. Bernardo, F. T. Oliveira, and J. C. Sousa, "Forecasting Heating and Cooling Energy Demand in an Office Building using Machine Learning Methods," in 2020 International Young Engineers Forum (YEF-ECE). IEEE, 2020.

[33] J. Badenhorst, "Utilising mine-cooling auxiliaries for optimal performance during seasonal changes," M.Eng Dissertation, North-West University, Potchefstroom, 2022.

[34] I. Schuin, "Evaluating different statistical regression models for industrial energy measurement and verification," M.Eng Dissertation, North-West University, Potchefstroom, 2019.

[35] A. Abdullah, A. Joseph, A. Kandeal, W. H. Alawee, P. Guilong, A. K. Thakur and S. W. Sharshir, "Application of machine learning modeling in prediction of solar still performance: A comprehensive survey," Results in Engineering, vol. 21, 2024.

[36] J. Moolayi, Learn Keras for Deep Neural Networks, Vancouver: Apress, 2019.

[37] I. H. Sarker, "Machine Learning: Algorithms, Real-World Applications and Research Directions," SN Computer Science, vol. 160, pp. 2-21, 2021.

[38] M. C. Furumele, "Dynamic control of mine cooling systems using artificial intelligence," M.Eng Dissertation, North-West University, Potchefstroom, 2023.

[39] "ASHRAE Guideline: Measurement of energy, demand, and water savings: ASHRAE Guideline 14," 2014.